Supporting Information

Targeted Design and Synthesis of a Highly Selective Mo-based Catalyst for the Synthesis of Higher Alcohols

Wei Xie,[a] Jilong Zhou,[a] Lili Ji,[a] Song Sun,*[ab] Haibin Pan,[a] Junfa Zhu,[a] Chen Gao,*[ab] and Jun Bao*[ab]

[a] National Synchrotron Radiation Laboratory, Collaborative Innovation Center of Chemistry for Energy Materials, University of Science and Technology of China, Hefei, Anhui 230029 (P. R. China)

[b] CAS Key Laboratory of Materials for Energy Conversion, Department of Materials Science and Engineering, University of Science and Technology of China, Hefei, Anhui 230026 (P. R. China)

*E-mail: suns@ustc.edu.cn; cgao@ustc.edu.cn; baoj@ustc.edu.cn.

Experimental

Catalyst synthesis

All chemicals with the A.R. grade were purchased from *Sinopharm Chemical Reagent* Co., Ltd, and were used as received without purification. The catalysts were prepared by a sol-gel method using citric acid as a complexant. A typical procedure is as follows: First, 4.63 g $(NH_4)_6Mo_7O_{24}\cdot 4H_2O$ and 3.82 g $Co(NO_3)_2\cdot 6H_2O$ were dissolved in 12 ml and 8 ml deionized water, respectively. The $Co(NO_3)_2$ aqueous solution was added dropwise to the $(NH_4)_6Mo_7O_{24}\cdot 4H_2O$ aqueous solution under stirring. The molar ratio of Co/Mo was 0.5. And then a calculated amount of 50 wt% $Mn(NO_3)_2$ aqueous solution was added to the solution above. The molar ratios of Mn/Mo were 0.00, 0.05, 0.10, 0.15, 0.20 and 0.25, respectively. A certain amount of citric acid aqueous solution was added slowly into the mixed solution under constant stirring. The molar ratio of citric acid to metallic ions was 0.4. Finally, the K_2CO_3 aqueous solution containing a calculated amount of K was added dropwise to the mixed solution. After adjusting the pH value of the solution to 3.5, the mixed solution was kept in a water bath at 343 K until the gel was formed. The as-prepared gel was dried at 393 K for about 15 h and then calcined in flowing nitrogen at 673 K for 4 h. All samples were ground, pressed, crushed, and sieved through 40-60 mesh prior to loading in the reactor for the catalytic performance evaluation.

Catalyst characterization

Transmission electron microscopy (TEM), selected area electron diffraction (SAED) and scanning transmission electron microscopy combined with energy-dispersive X-ray spectroscopy (STEM-EDS) mapping measurements for the catalyst samples were performed on a JEOL JEM-2100F field-emission transmission electron microscope with an accelerating voltage of 200 kV. High-resolution transmission electron microscopy (HR-TEM) images were obtained from a JEOL JEM-2010 high-resolution transmission electron microscope operating at 200 kV accelerating voltage.

Powder X-ray diffraction (XRD) patterns were carried out on a Rigaku TTR-III X-ray diffractometer with Cu Kα (λ=0.15418 nm) radiation operated at 40 kV and 200 mA .

X-ray photoelectron spectroscopy (XPS) measurements were collected on an ESCALAB 250 X-ray photoelectron spectrometer with Al Kα ($h\nu$=1486.6 eV) radiation.

In situ synchrotron radiation XPS experiments were carried out at the Photoemission Endstation at BL10B beamline in the National Synchrotron Radiation Laboratory (NSRL), at the University of Science and Technology of China (USTC). The samples were pressed into thin pellets and then placed into the reaction cell and reduced in a flowing H_2 under atmospheric pressure at 673 K for 4 h. Then the samples were cooled down to room temperature and transferred to the analysis chamber under vacuum conditions for measurements.

The X-ray absorption spectra (XAS) measurements were performed at the 1W1B beamline of Beijing Synchrotron Radiation Facility (BSRF), China. The electron storage ring was operated at 2.5 GeV with an average current of 200 mA. All data of absorption samples were collected in transmission mode. The energy of the absorption spectra at Mo K-edge and Co K-edge were calibrated by measuring the XANES of a Mo metal foil and Co metal foil.

Catalytic performance evaluation

The catalytic performance for higher alcohol synthesis from syngas was performed in a fixed-bed pressurized reaction system equipped with a stainless steel reactor tube (8 mm internal diameter). For each experiment, 0.5 g catalyst, which was diluted with quartz sand to make a total volume of 2 ml, was loaded at the center of the reactor tube. The temperature was monitored with a thermocouple inserted in the catalyst bed. Prior to the reaction, the catalysts were reduced in a flow of pure H_2 at a flow rate of 40 mL/min under atmospheric pressure for 12 h. Then the reactor was cooled down to reaction temperature and feed gas (30% CO, 60% H_2 and 10% N_2)

was introduced into the reactor. The effluent gas was cooled in an ice-water bath to separate into gas and liquid phases under the reaction pressure. The CO, CO_2 and CH_4 in effluent gas were analyzed on an on-line thermal conductivity detector (TCD, KeXiao, GC-1690) equipped with a 3 m TDX-01 packed column. Hydrogen was used as the carrier gas. The gaseous hydrocarbons were analyzed on an on-line flame ionization detector (FID, KeXiao, GC-1690F) equipped with a 3 m Porapak Q packed column using N_2 as the carrier gas. 1.01% CH_4 was used as standard gas for calculating the composition of hydrocarbons. Liquid products were collected for an appropriate period and then analyzed on the same FID by injection. The alcohols distribution was calculated from the peak area using a standard liquid of mixed alcohol. H_2O content in liquid products was analyzed by a moisture meter (ANTING, ZSD-2). Because the higher alcohol synthesis from syngas requires an induction period to reach steady state, all activity data in this study were measured after the reaction was performed for 24 h.

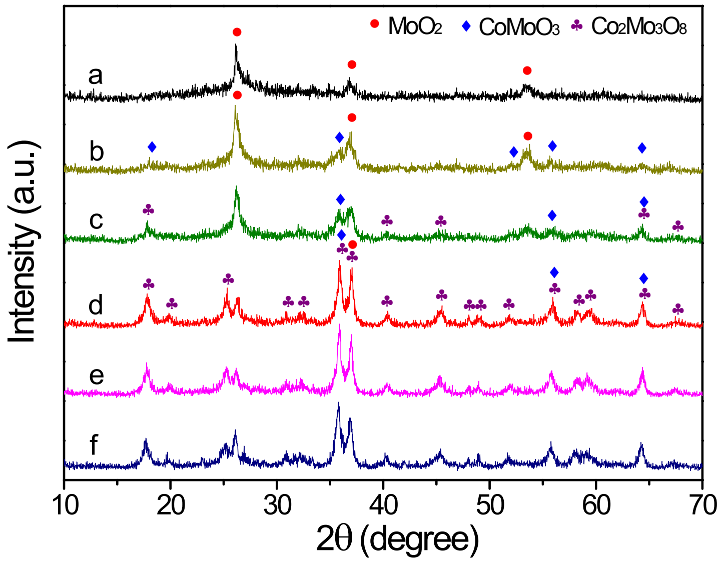

Figure S1. Powder XRD patterns of the fresh catalysts with different Mn/Mo molar ratio. (a) 0.00, (b) 0.05, (c) 0.10, (d) 0.15, (e) 0.20, (f) 0.25.

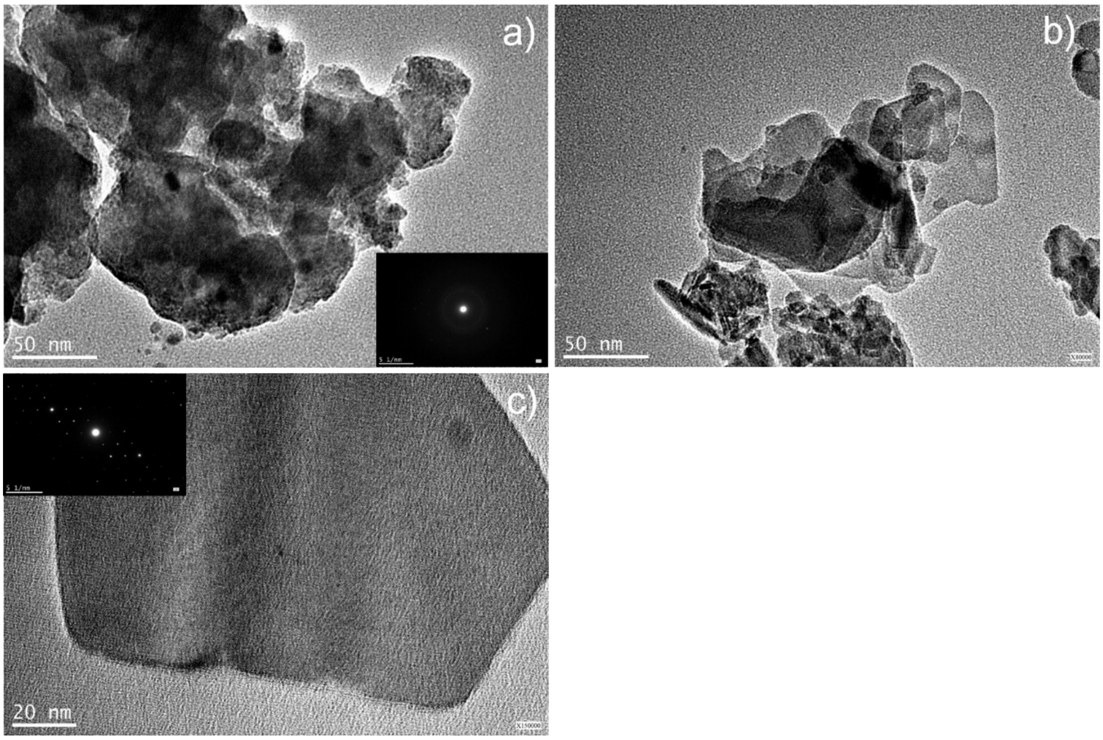

Figure S2. Representative TEM images of (a) Mn-free catalyst and (b), (c) Mn-doped catalyst with Mn/Mo ratio of 0.15 at different magnification. The insets show the electron diffraction patterns.

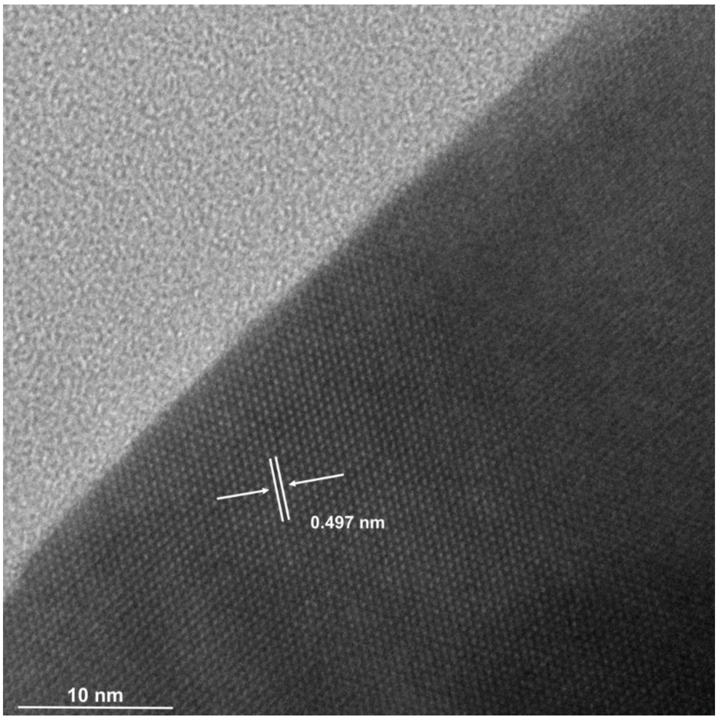

Figure S3. HR-TEM image of Mn-doped catalyst with Mn/Mo ratio of 0.15. The crystal lattice fringes are clearly visible and the observed lattice spacing of 0.497 nm is in agreement with the *d* value of {002} facet of $Co_2Mo_3O_8$ crystal lattice.

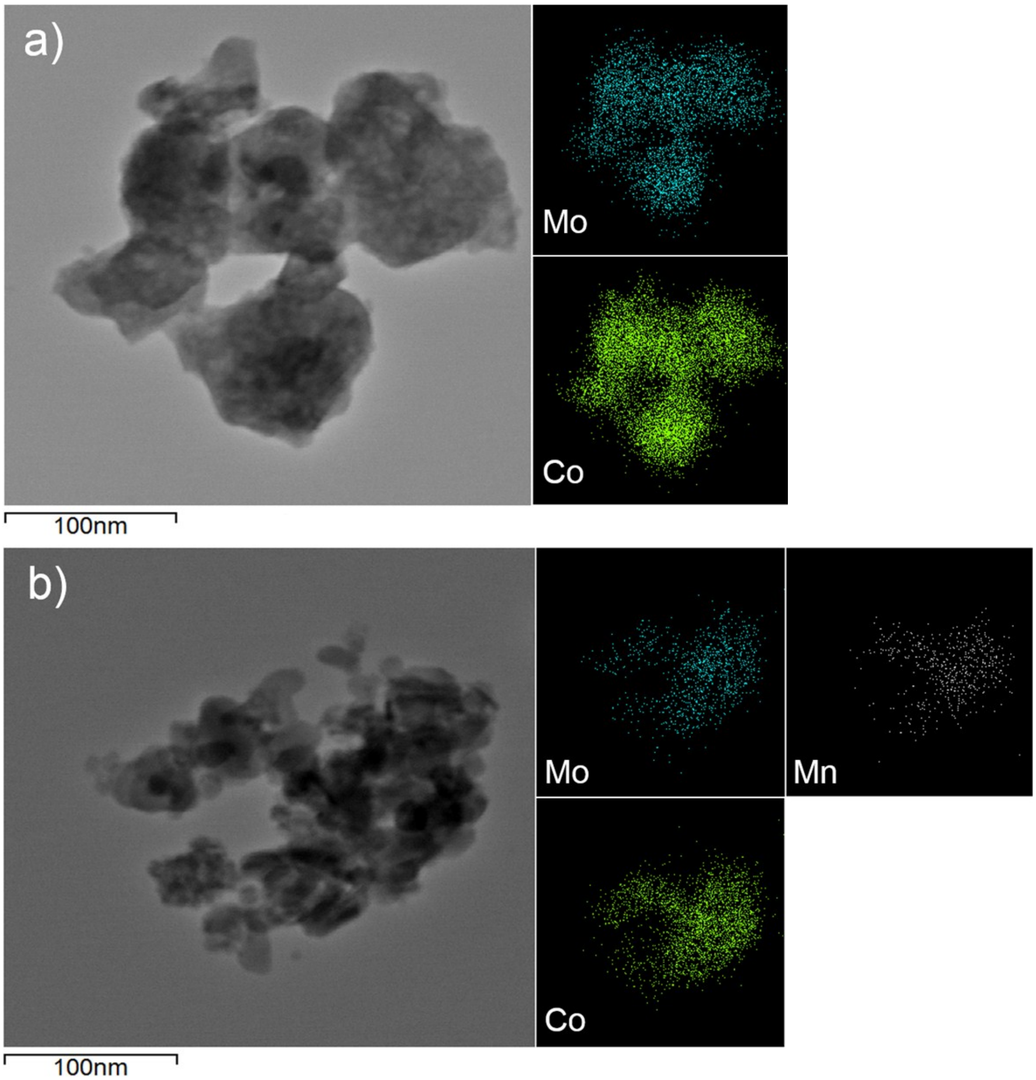

Figure S4. STEM and corresponding elemental mapping images of the fresh catalysts. (a) Mn/Mo=0.00, (b) Mn/Mo=0.15.

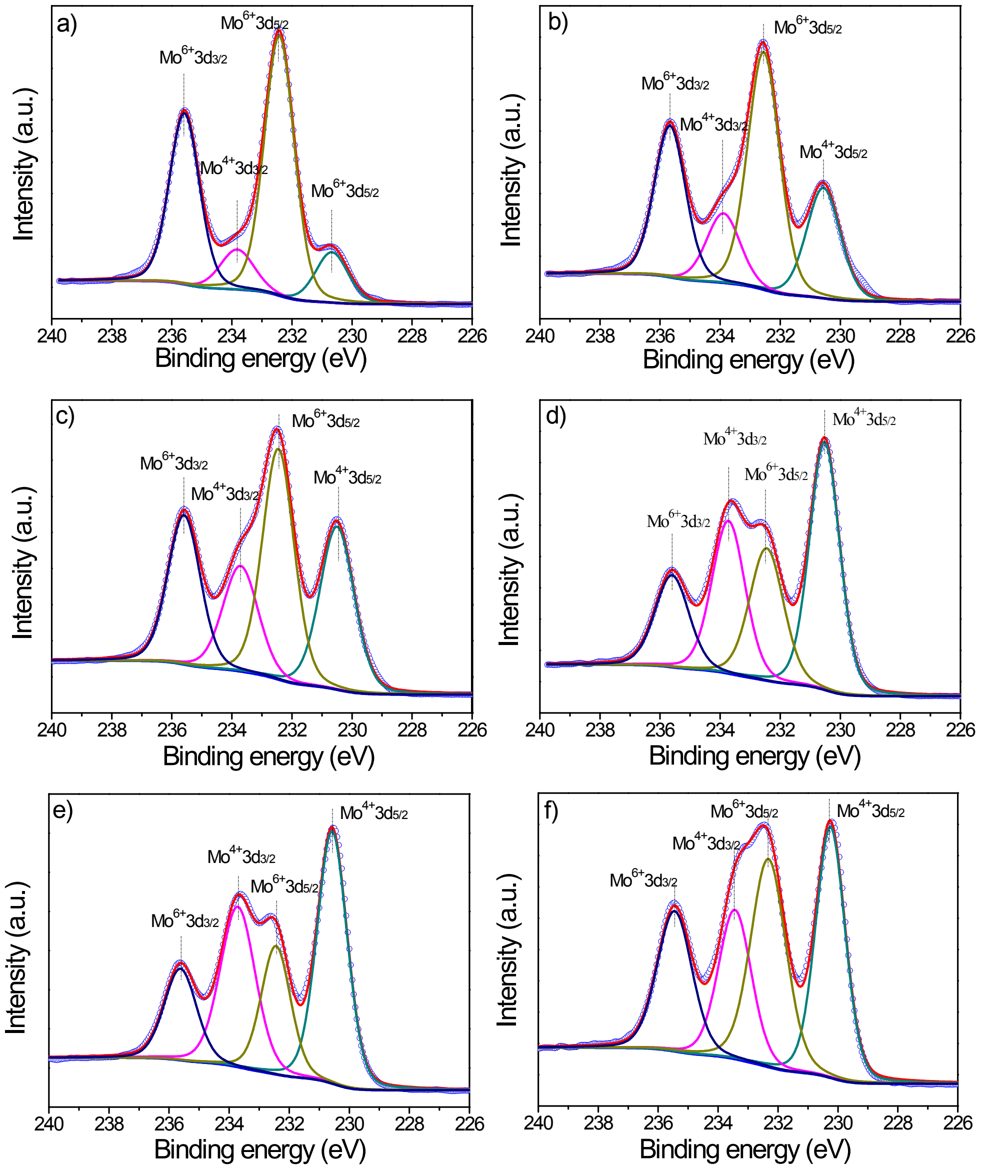

Figure S5. XPS spectra of Mo 3d for the fresh catalysts with different Mn/Mo molar ratio. (a) 0.00, (b) 0.05, (c) 0.10, (d) 0.15, (e) 0.20, (f) 0.25.

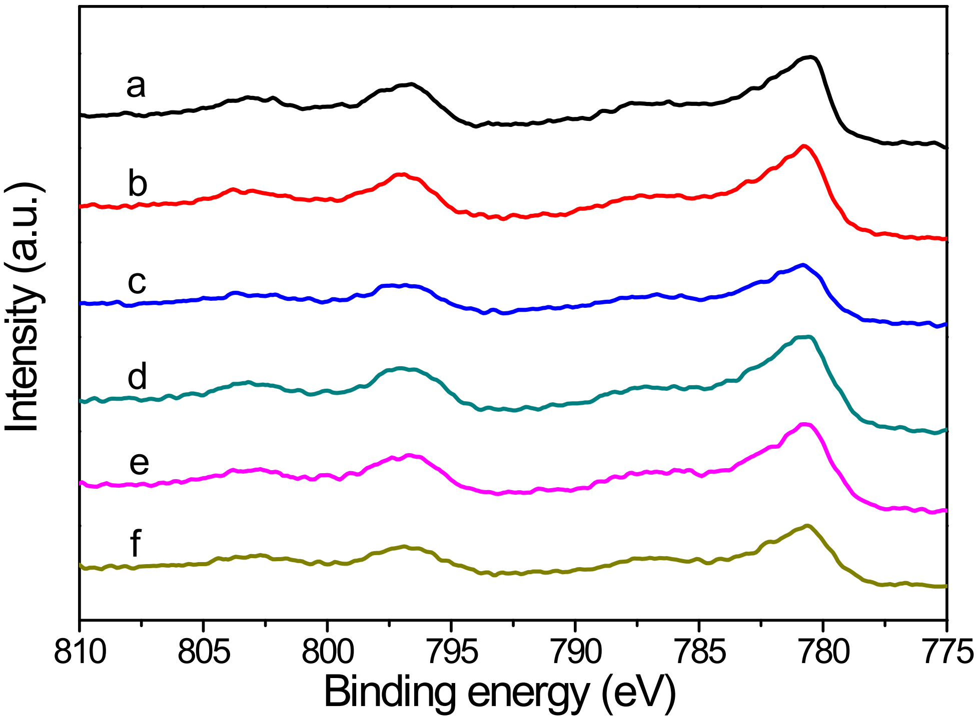

Figure S6. XPS spectra of Co 2p for the fresh catalysts with different Mn/Mo molar ratio. (a) 0.00, (b) 0.05, (c) 0.10, (d) 0.15, (e) 0.20, (f) 0.25.

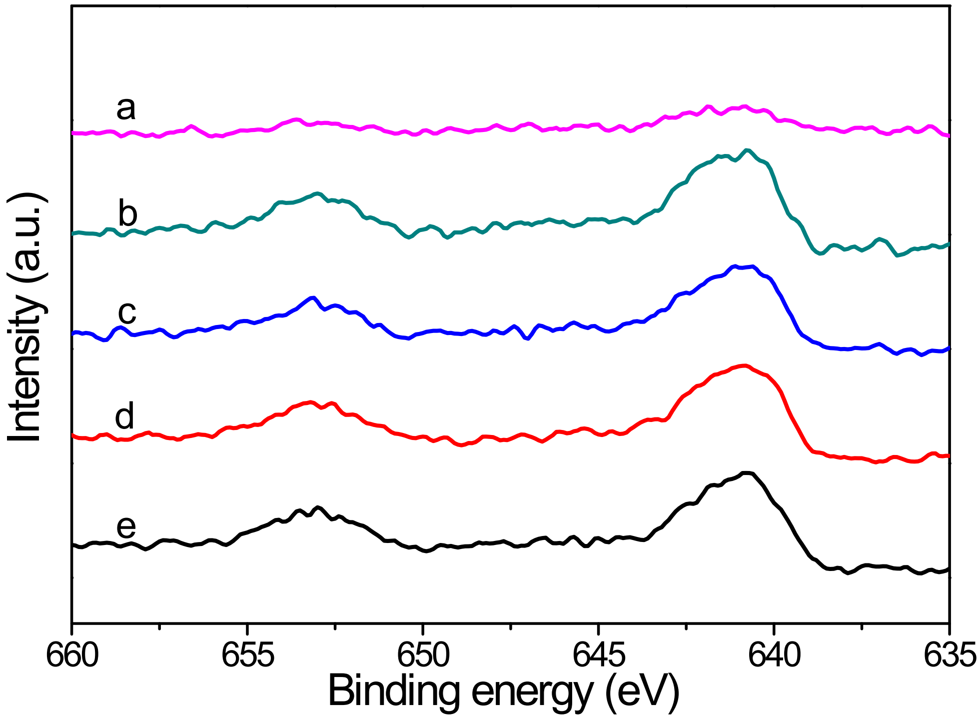

Figure S7. XPS spectra of Mn 2p for the fresh Mn-promoted catalysts with different Mn/Mo molar ratio. (a) 0.05, (b) 0.10, (c) 0.15, (d) 0.20, (e) 0.25.

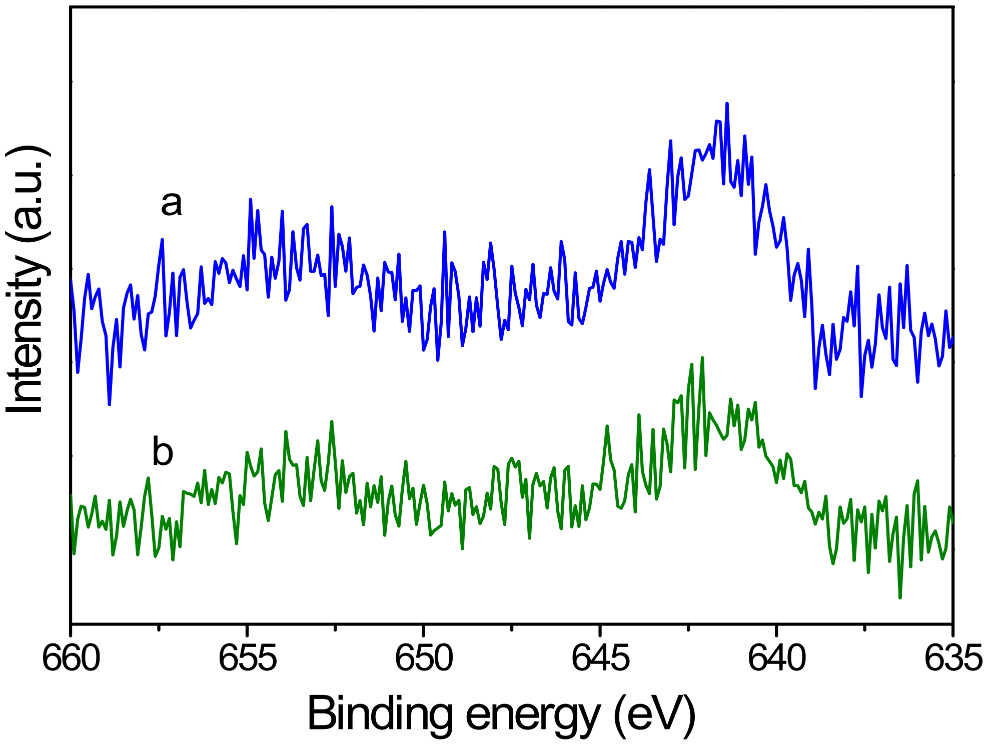

Figure S8. In-situ synchrotron radiation XPS spectra of Mn 2p for the catalyst with Mn/Mo molar ratio of 0.15. (a) the fresh catalyst, (b) the reduced catalyst.

Table S1. Distribution of surface Mo species of the fresh catalysts from the XPS data.

Sample (Mn/Mo)	Mo^{6+}			Mo^{4+}		
	$3d_{5/2}$ (eV)	$3d_{3/2}$ (eV)	Percentage (%)	$3d_{5/2}$ (eV)	$3d_{3/2}$ (eV)	Percentage (%)
0.00	232.4	235.6	82.5	230.6	233.8	17.5
0.05	232.5	235.6	67.9	230.6	233.8	33.1
0.10	232.4	235.6	56.6	230.5	233.7	43.4
0.15	232.4	235.6	37.7	230.5	233.7	62.3
0.20	232.4	235.6	33.3	230.6	233.7	66.7
0.25	232.3	235.5	49.8	230.4	233.6	50.2